

# Systematic Study of Low Loss Amorphous Core Transformers: Design and Testing

Chang-Hung Hsu<sup>a,b</sup>, Yeong-Hwa Chang<sup>a</sup>

<sup>a</sup> Electrical Engineering, Chang Gung University, Tao-Yuan, Taiwan

<sup>b</sup> Electric Machine, Fortune Electric Ltd, Co., Tao-Yuan, Taiwan

E-mail: [chshiu@fortune.com.tw](mailto:chshiu@fortune.com.tw)

*Abstract:* - A comprehensive study on the amorphous alloy core transformer is presented in this paper, where a single-phase 25kVA transformer with Fe-based amorphous alloy core is considered. The procedures about the design and implementation of the amorphous core transformer are discussed in detail. According to the measured results, the lowest core loss occurs with an annealing temperature 360°C under a dc magnetic field density 800A/m. Besides, no load test, sudden short circuit test, and lightning impulse test are performed to ensure the transformer performance. Finally, at the same specifications and rated power, experimental results are presented for the amorphous alloy SA1 core transformer and traditional silicon steel core transformer. It can be seen that the amorphous core transformer can provide better performance in the aspect of core loss and exciting power.

*Key-Words:* - Amorphous materials; Transformer design; Core loss; Exciting power; Annealing

## 1 Introduction

In the last decade, due to the remarkable capability of low loss, amorphous alloys have been utilized as core materials in the aspects of energy saving and CO<sub>2</sub> discharge reduction. As the amorphous cored distribution transformers, the advantages are that low magnetic hysteresis loss and low eddy current loss associated with a small magnetic anisotropy and a large resistivity. However, the disadvantages to be known are lower saturation magnetic induction, thermal instability, mechanical brittleness and low stacking factor [1, 2]. Due to the progress of physical and magnetic techniques, the soft ferromagnetic materials have many excellent properties of high saturation magnetic flux density, high permeability and low losses [3, 4]. The Fe-based amorphous alloys, nanocrystalline Fe-Si-B-Nb-Cu alloy and NANOPERM (R) Fe-M-B (M=Zr, Hf, Nb) alloys with higher saturated magnetic flux density are suitable for low frequency application such as power transformer and choke coils for active filters for power supplies [5, 6]. However, the materials of the Mn-Zn ferrite with low permeability are not suitable for high frequency applications, such as thin film inductors and transformers for micro switching converter for electric equipment [7, 8]. Furthermore, Co-based amorphous alloys and Fe-Ni alloy do have the advantages of high permeability and low losses, nevertheless, low saturated magnetic flux density is the main drawback, and it is hard and expensive to be acquired [9, 10].

In [11, 12], it is concluded that Fe-based amorphous alloys may have unique core magnetic permeability, magnetic flux density and hysteresis loop along with different compositions. Also, subject to different composition elements, the magnetic properties of alloys will be different as well, and the annealing temperature control will result in their related material losses. The amorphous alloy is a magnetic material and the ribbon is usually with the thickness of 0.02~0.03 mm. In practice, amorphous metals are metallic materials with a nanocrystalline liquid-like molecular structure. These metals are formed in long and thin strips by rapidly cooling molten metal to prevent crystallization of the material during solidification. Compared with silicon steel, the soft ferromagnetic metals have lower losses and lower CO<sub>2</sub> discharge. However, because of its hardness and thickness, the manufacturing surface of amorphous alloy core exists uneven surface, thus the associated stacking factor is only 0.85+ while the stacking factor of silicon steel is 0.95+. Because of the stress resulted from manufacturing process, annealing process is required for the amorphous alloy core to improve the magnetic characteristic. In [13], a 1kVA transformer of amorphous alloy is manufactured. To process the annealing temperature control, the annealing temperature is set to be 380°C with an applied direct current magnetic flux density 800A/m, so that the best core crystallization point can be obtained.

The rest of this paper is organized as follows. In section 2, the transformers design, manufacturing, annealing and testing are discussed in detail. In

section3, the measured results of best core annealing temperature process, transformer loss, sudden short circuit test and lightning impulse test are performed to ensure the amorphous-core transformer performance, compared with traditional silicon steel (23ZDMH90) core transformers. The conclusion is given in section 4.

## 2 Application of a single-phase transformer

### 2.1 Winding design

During the process of transformer design and manufacturing, winding and core design are two indispensable factors to be investigated in advance. Practically, for the design of winding, the winding loss is determined by the rated currents, current density, winding material, cross-section area and turn ratio. This paper presents the design and implementation of a single-phase Fe-based amorphous alloy core transformer with capacity of 25kVA, primary/secondary voltage of 6.9kV/0.24-0.12kV, and 60 Hz. This paper presents the design and implementation of a single-phase Fe-based amorphous alloy core transformer with capacity of 25kVA, primary/secondary voltage of 6.9kV/0.24-0.12kV, and 60 Hz. The cross-section areas of the primary and secondary windings, wound with copper wire and copper sheet windings conductor, are  $A_p$  and  $A_s$  including insulation, respectively, and the relative current density are  $J_p$  and  $J_s$  and winding conductor are  $T_p$  and  $T_s$  turns, respectively. The specifications of winding are summarized in Table 1.

In the design of transformer cores, some factors have to be considered such as the cross-section area and magnetic flux density of cores, the stacking factor, and core windows, where the specifications of amorphous alloy ribbon and core are shown in Fig. 1. The thickness of amorphous alloy ribbon metal is smaller than that of conventional silicon steel. In general, the thickness of a piece of silicon steel is about 0.3 mm or higher, however, it is only approximately 0.025 mm (1mils) for the amorphous alloy ribbons. For the sake of lower thickness and higher hardness, the surface of amorphous alloy core will be more likely uneven compared with silicon steel core. The effect of stacking factor, about 0.85+ for amorphous alloy core and 0.95+ for silicon steel core, should be considered in the later. In Fig 1(b), the core dimension of length and width are  $A$  and  $B$ , in which  $C$  is the stacking width,  $D$  is the ribbon width, and the radius of circular factor is  $R$ , respectively.

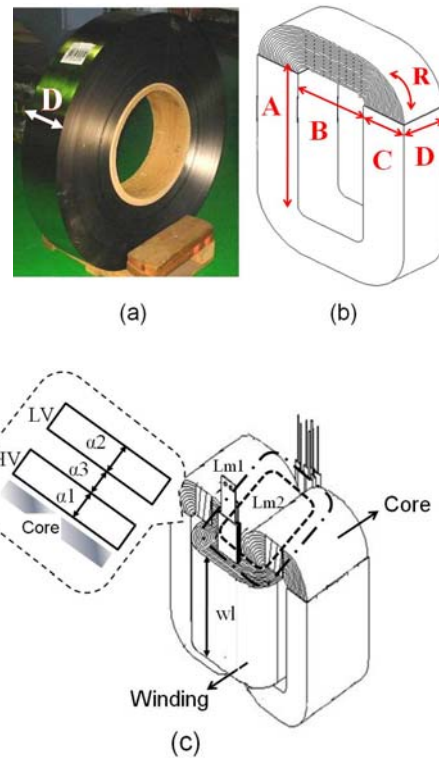


Fig. 1. The sketch of the transformer design (a) Ribbon, (b) Core, (c) Winding distribution.

The core cross-section area of core is calculated as

$$A_c = \frac{10^4}{4.44 \times B_m \times f \times \delta} \cdot \frac{V}{N} \quad (1)$$

where  $f$  is the power frequency,  $B_m$  is magnetic flux density in tesla,  $\delta$  is core stacking factor, the  $V/N$  is volts per turn ratio, respectively.

The Fig. 1(a) is show winding distribution diagram. The voltage per turn of the winding is calculated as

$$\frac{V}{T} = \left\{ \frac{0.395 \times T_c \times \left( \frac{\alpha_1 + \alpha_2}{3} + \alpha_3 \right) \times \left( \frac{L_{m1} + L_{m2}}{2} \right)}{S \times \%IX \times Wl} \times \frac{\left( \frac{\alpha_1 + \alpha_2 + \alpha_3}{Wl \times \pi} - 1 \right)}{100} \times 2f \right\}^{\frac{1}{2}} \quad (2)$$

Where  $S$  is the number of phase,  $\alpha_1$  is rolling thickness of primary winding,  $\alpha_2$  is rolling thickness of secondary voltage,  $\alpha_3$  is insulation space between primary and secondary winding,  $L_{m1}$  is average length of inside winding,  $L_{m2}$  is average length of

outside winding,  $f$  is operation frequency,  $Wl$  is winding high, respectively.

## 2.2 Core Loss

The core loss  $P_c$  is calculated as

$$P_c = P_{\text{watt/kg}} \times G_{ei} \times D.F. \quad (3)$$

where  $P_{\text{watt/kg}}$  is the watt per unit ribbon, depending on the core operation frequency, and  $G_{ei}$  is the core weight. It is noted that the core loss will be slightly higher than its rated value of ribbon because of the process of cutting and crimping. In this paper, particularly,  $D.F.$  is defined as the core destroy factor, 1.1~1.3. The weight of core is calculated as

$$G_{ei} = C \times D \times l_i \times \rho \times \delta \times 10^{-6} \quad (4)$$

where  $l_i$  is the circumference along uneven surface,  $\rho$  is the gravity of core material, 7.2 g/cm<sup>3</sup> of amorphous alloy and 7.65 g/cm<sup>3</sup> of silicon steel.



Fig. 2. Overview of 25 kVA single phase transformer.

## 3 Fabrication and Testing

### 3.1 Core Loss and Magnetic Characteristics

The annealing temperature control is crucial for the manufacturing of amorphous materials. If the annealing temperature is too high, it will cause localized partial crystallization, and the resulting magnetic crystalline anisotropy will tend to increase the core loss. Otherwise, if the annealing temperature is too low; the residual stress is not adequately relieved. From experimentation results, for the amorphous alloy SA1 ribbon, the annealing temperature is set at 360°C for one hour in nitrogen atmosphere. During the annealing process, a DC current driven magnetic field is applied to further improve the magnetic

properties. In this paper, the magnetic field density 800 A/m is utilized to reduce the core loss.

In Fig. 4, according to experimentation results, it can be found that to obtain the lowest core loss the annealing temperature is of 360±10°C for the amorphous alloy SA1 core. The measured core loss and exciting power related to magnetic induction are shown in Fig. 5 and Fig. 6, it can be seen that the core loss of SA1 core transformer is less than the value of silicon steel transformer with each designated magnetic flux density  $B_m$ . In Fig. 6, the saturated flux density of SA1 transformer is about 1.56 (T), while the saturated flux density of silicon steel transformer is about 2.0 (T).

Table 1 Design parameters of transformer

Specification	Description P: primary, S: secondary		Unit
	Amorphous Alloy(SA1)	Silicon Steel (23ZDMH90)	
Capacity	25	25	kVA
Voltage, $V_p/V_s$	6900/240	6900/240	V
Current, $I_p/I_s$	3.623/104.2	3.623/104.2	A
Winding			
Conductor cross section area, $A_p/A_s$	2.0×2.0/0.4×230	1.7×1.7/0.4×175	mm <sup>2</sup>
Current density, $J_p/J_s$	1.26/1.13	1.59/1.49	A/mm <sup>2</sup>
Total turn number, $T_p/T_s$	1800/60	1260/42	Turn
Impedance voltage percentage, %IZ	2.14	2.29	%
Winding resistance, $R_p/R_s$	9.247/8.68×10 <sup>-3</sup>	8.232/7.24×10 <sup>-3</sup>	Ω
Winding loss, $P_w$	240	224	W
Core			
Core height, A	260	205	mm
Core width, B	120	69	mm
Staking width, C	80	41	mm
Ribbon width, D	170	180	mm
Radius circular Factor, R	6.4	4.8	
Magnetic flux density, $B_m$	1.3164	1.5378	T
Core loss, $P_c$	26	64	W

It is notice that the exciting power of SA1 transformer is less than that of silicon steel transformer with magnetic flux density  $B_m$  less than 1.33 (T). To achieve better efficiency by using the fabricated SA1 amorphous alloy core transformer, it is suggested to follow the observation that the magnetic flux density is less than 1.33 (T).

### 3.2 Sudden short circuit test

The sudden short-circuit tests, shown in Fig. 7, are proceeded with the secondary side shorted, in which the primary exciting current is 40 times of its rated value for at least 780 ms. It can be seen that, the desired IEEE standard is satisfied, and there is no demolishment occurrence in mechanical phenomenon after retesting.

### 3.3 Lightning impulse test

Before performing the lightning impulse test, it is required with the secondary side shorted and core grounded. According to the IEEE specifications, the input test waves include full-wave voltage -95kV, reduced full-wave voltage, and chopped-wave voltage -110kV, where the impulse waveform is  $1.2 \times 50 \mu s$ . Especially, the test time of the chopped-wave case should be more than  $1.8 \mu s$ . The complete lightning impulse test consists of three steps, reduced full-wave impulse test one time, chopped-wave impulse test twice, and full-wave impulse test one time. Experimental results are shown in Fig. 8, where (a)–(d) are for amorphous alloy core and (e)–(h) are for silicon steel core, respectively. Obviously, form Fig. 8, there is no breakdown occurrence caused by impulse waves test, and the IEEE standard is satisfied as well.

## 4 Conclusion

This paper presents the design and implementation of a single-phase Fe-based SA1 amorphous alloy core transformer with capacity of 25 kVA, primary/secondary voltage of 6.9kV/0.24-0.12kV, and 60 Hz. The annealing temperature is set to be 360 °C applied with a DC current 800 A/m magnetic field so that the lowest core loss of best crystallization can be obtained. Following the IEEE standards, no load test, sudden short circuit test, and lightning impulse test are performed to ensure the transformer performance. Experimental results illustrate that all the required specifications are satisfied. Also,

compared with silicon steel transformer, the constructed amorphous alloy core transformer has lower core loss and better stability performance.

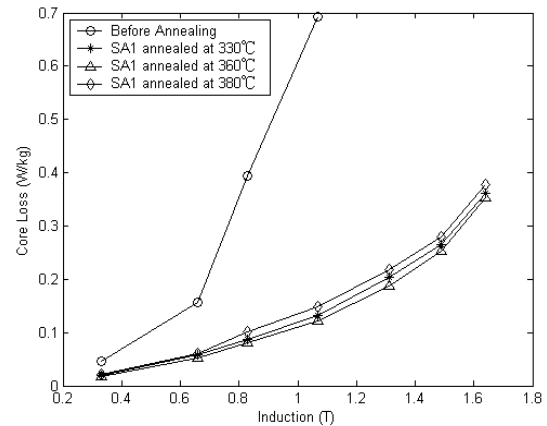


Fig.4. The measured core losses of SA1 core transformer with respect to different annealing temperatures

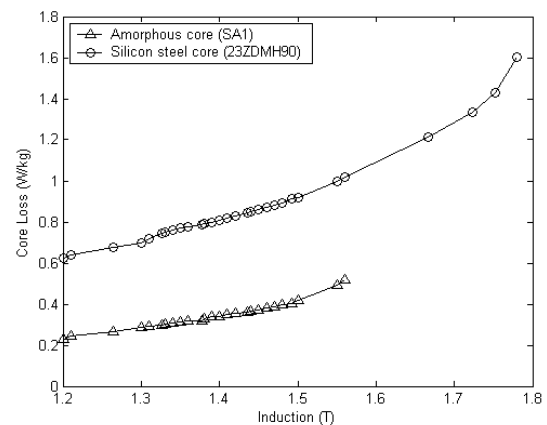


Fig.5. The measured core losses of SA1 core transformer and silicon steel transformer.

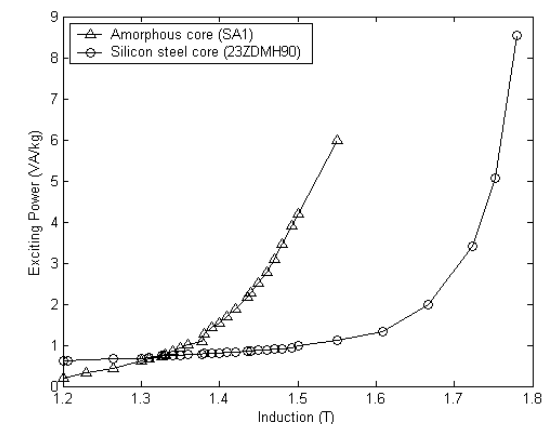


Fig.6. The measured exciting power responses of SA1 core transformer and silicon steel transformer.

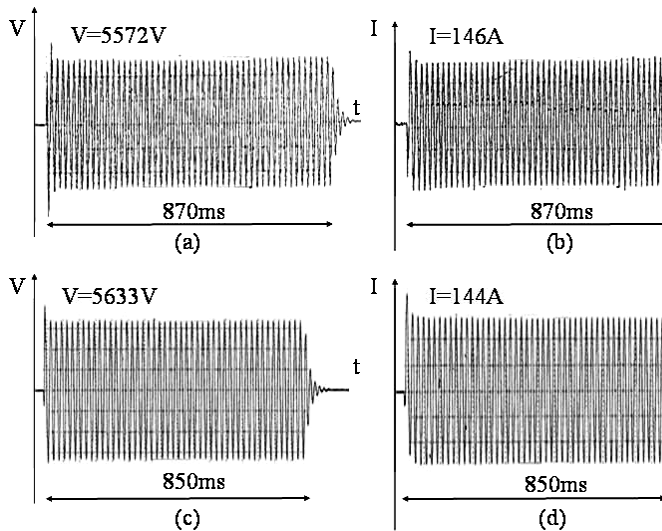


Fig. 7. Sudden short circuit test: (a) and (b) for amorphous alloy core; (c) and (d) for silicon steel.

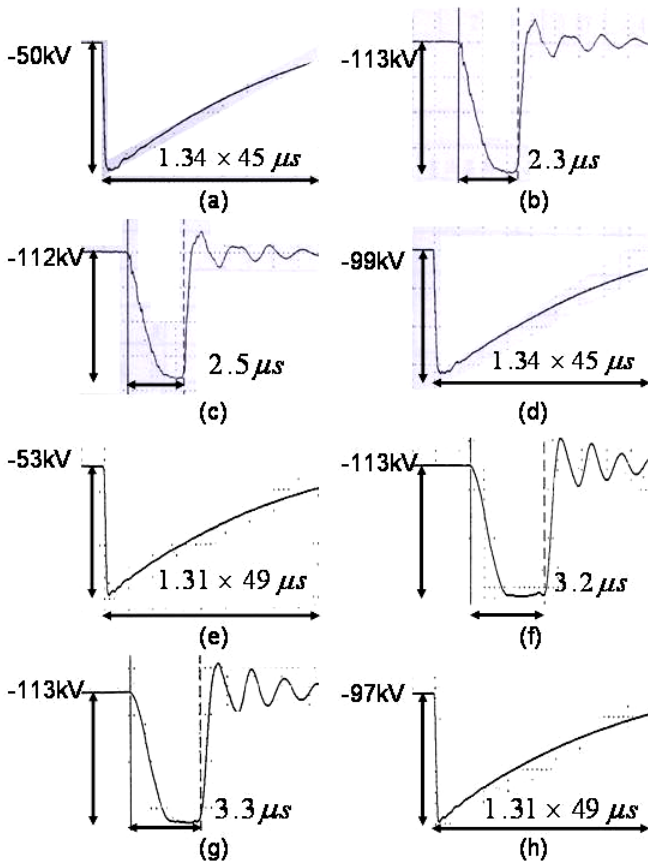


Fig. 8. Lightning impulse tests: (a)-(d) for amorphous alloy core, reduced full-wave test one time, chopped-wave test twice, and full-wave test one time, respectively; (e)-(h) for silicon steel core, reduced full-wave test one time, chopped-wave test twice, and full-wave test one time, respectively.

References:

[1] S. Ezure, Y. Imai, H. Sato, S. Yamada, K. Yamanaka, S. Saito, Long-term reliability of amorphous alloy wound core distribution transformers, *IEEE Transaction on Power Delivery*, Vol.9, No.1, 1994, pp. 249–256.

[2] R. Hasegawa, Applications of amorphous magnetic alloys, *Material Science Engineer A*, Vol.375-377, No.15, 2004, pp. 90–97

[3] U. D. Annakkage, P. G. McLaren, E. Dirks, R. P. Jayasinghe, A. D. Parker, A current transformer model based on the Jiles-Atherton theory of ferromagnetic hysteresis, *IEEE Transaction on Power Delivery*, Vol.15, No.1, 2000, pp.57–61

[4] A. Sharma, S. Acharya, T. Vijayan, P. Roychoudhury, P. H. Ron, High-frequency characterization of an amorphous magnetic material and its use in an induction adder configuration, *IEEE Transaction on Magnetics*, Vol.39, No.2, 2003, pp. 1040–1045.

[5] A. Makino, T. Hatanai, Y. Naitoh, T. Bitoh, Applications of nanocrystalline soft magnetic Fe-M-B (M=Zr, Nb) alloys “NANOPERM(R)”, *IEEE Transaction on Magnetics*, Vol.33, No.5, 1997, pp. 3793-3798.

[6] C. Dudek, A. L. Engelvin, O. Acher, Static and dynamic properties of Fe-Si-B-Nb-Cu nanocrystallized ferromagnetic glass-coated microwires from 20°C to 350°C, *IEEE Transaction on Magnetics*, Vol.42, No.10, 2006, pp. 2787-2789.

[7] S. T. Liu, S. R. Huang, H. W. Chen, Using TACS functions within EMTP to set up current-transformer model based on the Jiles–Atherton theory of ferromagnetic hysteresis, *IEEE Transaction on Power Delivery*, Vol.22, No.4, pp.2222-2227.

[8] R. Huang, D Zhang, Experimentally verified Mn–Zn ferrites' intrinsic complex permittivity and permeability tracing technique using two ferrite capacitors, *IEEE Transaction on Magnetics*, Vol.43, No.3, 2007, pp. 974-981.

[9] S. Sandacci, D. Makhnovskiy, L. Panina, V. Larin, Stress-dependent magnetoimpedance in Co-based amorphous wires with induced axial anisotropy for tunable microwave composites, *IEEE Transaction on Magnetics*, Vol.41, No.10, 2005, pp. 3553-3555.

[10] K. Y. HE, Y. H. Zhao, G. G. YH, L. Z. Cheng, B. LZ, B. Wu, M. L. Sui, W. Z. Chen, Studies of crystallization and soft magnetic properties of FeNiMoB(Si) alloys, *Journal of Magnetism and Magnetic Materials*, Vol.316, No.1, 2007, pp. 34-39.

- [11]B. Peng, W. L. Zhang, Q. Y. WL, Q. Y. Xie, H. C. Jiang, W. X. Zhang, Y. R. WX, Study on the magnetic domain and anisotropy of FeCoSiB amorphous films fabricated by strained growth method, *Journal of Magnetism and Magnetic Materials*, Vol.318, No.1-2, 2007, pp. 14-17
- [12]M. Dobromir, M. Neagu, G. Popa, H. Chiriac, V. Pohoățã, C. Hison, Surface and bulk magnetic behavior of Fe–Si–B amorphous thin films. *Journal of Magnetism and Magnetic Materials*, Vol.316, No.2, pp.904-907.
- [13]B. A. Luciano, M. E. de Morais, C. S. Kiminami, Single phase 1-kVA amorphous core transformer: design, experimental tests, and performance after annealing. *IEEE Transaction on Magnetics*, Vol.35, No.4, 1999, pp. 2152-2154.